applied optics

Widely tunable external-cavity surface-emitting laser using various methods

LIN MAO,[1] XIAOJIAN ZHANG,[1] RENJIANG ZHU,[1] TAO WANG,[1,3] LIJIE WANG,[2] AND PENG ZHANG[1,4]

[1]College of Physics and Electronic Engineering, Chongqing Normal University, Chongqing 401331, China
[2]State Key Laboratory of Luminescence and Applications, Changchun Institute of Optics, Fine Mechanics and Physics, Chinese Academy of Sciences, Changchun, Jilin 130033, China
[3]e-mail: wangt@cqnu.edu.cn
[4]e-mail: zhangpeng2010@cqnu.edu.cn

Received 14 June 2021; revised 4 July 2021; accepted 7 July 2021; posted 8 July 2021 (Doc. ID 432133); published 30 July 2021

We report a widely tunable optically pumped vertical-external-cavity surface-emitting laser. The multiple quantum wells in the active region of the gain chip are generally designed to form the resonant periodic gain structure, and three different methods are used to tune the oscillating wavelength. The maximum wavelength coverage of 45 nm is obtained when a 2 mm thickness birefringent filter is introduced in a straight-line cavity, while the tuning range of 8 nm is performed by employing a 0.15 mm thickness uncoated Fabry–Perot etalon. For the first time, to the best of our knowledge, we present an 11 nm tuning range by the use of an inserted blade as the tuning element, and the related wavelength tuning mechanism is analyzed.

https://doi.org/10.1364/AO.432133

1. INTRODUCTION

Tunable lasers have significant applications in free-space laser communications [1], optical sensing [2], lidar, laser medical treatment [3], environment monitoring [4], and so on. One important direction of development of tunable lasers is to introduce new technical means or novel structure design to achieve a wider tuning range and higher-precision wavelength tuning capability to expand the application fields of tunable lasers.

As an early developed tunable laser, tunable dye lasers have wide spectral cover and moderate tuning range. However, the toxic solvent in which the gain medium (i.e., some kind of organic dye) of a dye laser must be dissolved results in troublesome maintenance [5]. Meanwhile, photochemical and thermal decomposition of the gain medium make laser frequency unstable, with poor reliability and short life [6].

In comparison, solid-state lasers have compact structure, good reliability, and long life. At the same time, they can output high power [7] and good beam quality and also achieve single-frequency [8,9] and frequency-doubled [10] operation. Unfortunately, the emission wavelength of a solid-state laser is restricted by the doped ions in the gain medium [11], and its wavelength tuning range is very limited (Ti:sapphire lasers should be excluded). Furthermore, the stability of a solid-state laser is easily affected by the pump source, because the absorption band of active ions is very narrow, and the output of the laser is very sensitive to the shift of the pumping wavelength [12].

Thanks to the state-of-the-art semiconductor material, tunable semiconductor lasers are developing rapidly and have been widely used in atomic and molecular physics (such as atom cooling and Bose Einstein condensation), optical communication, precision laser spectroscopy, etc. It is well know that the emission wavelength of semiconductor lasers covers a wide range from ultraviolet to mid-infrared, which is much larger than that of dye lasers and solid-state lasers. Compared with tunable dye lasers and solid-state lasers, tunable semiconductor lasers also have the unique advantages of high efficiency, long life, and small size, and they have high integration capacity.

Technically speaking, it is difficult to obtain high power and good beam quality at the same time from a traditional electrically pumped semiconductor laser. The output power of a single edge-emitting semiconductor laser has exceeded 10 W, but the laser is multi-transverse mode with poor beam quality. Although a vertical-cavity surface-emitting laser (VCSEL) can produce ideal beam quality, its output power is limited to the magnitude of milliwatts due to its mode requirements.

Optically pumped vertical-external-cavity surface-emitting lasers (VECSELs), or named as semiconductor disk lasers (SDLs), combine advantages both of semiconductor surface-emitting lasers and solid-state disk lasers and can yield high power and good beam quality simultaneously [13–16]. The reported output power of a VECSEL with fundamental transverse mode was more than 20 W, and the M^2 factor of beam quality was about 1.1 [17]. The demonstrated maximum output power of a VECSEL has exceeded 100 W [18]. Based on the mature band engineering, the emission wavelength of VECSELs can be designed according to application needs. In addition, the

wavelength of VECSELs can be extended to a wide coverage from ultraviolet to mid-infrared if the technology of nonlinear frequency conversion is employed.

The flexible external-cavity structure and the typical gain bandwidth of more than 100 nm make VECSELs intrinsically suitable for tunable operation, and much work has been done successfully on tunable VECSELs at different wavebands and with various tuning ranges. In the 1000 nm waveband, the epitaxial growth of wafer is relatively well developed, and the applications of laser are relatively broad [19]. By using a birefringent filter (BRF) as the tuning element in a V-shaped cavity, a 20 nm tuning range around a center wavelength of 980 nm has been obtained [20], and this tuning range was extended to 33 nm in a two-chip VECSEL [21]. Through parametrically optimizing the layer structure of the gain element with respect to a target function specifying a desired unsaturated reflectance over a desired wavelength range, a continuously tunable wavelength between 967 and 1010 nm, corresponding to a tuning range of 43 nm, was reported [22]. By incorporating semiconductor quantum dots (QDs) in the active region of a laser, the effects of carrier confinement in all three dimensions offered additional broad gain bandwidth, and a 60 nm tuning range near the 1040 nm wavelength was realized [23]. Using only high reflecting mirrors, an 80 nm tuning region with lasing wavelength centered at 1034 nm was presented, and the authors attributed such wide tunability to the unique broad effective gain bandwidth of distributed Bragg reflector (DBR)-free SDLs achieved by eliminating the active mirror geometry [24]. By using only high-reflectivity mirrors in the resonator and controlling the active region temperature through readjustment of pump power and heat extraction, a record wide tunability of 95 nm was achieved at a 985 nm laser center wavelength [25]. However, it should be noticed that the 95 nm was the sum of the tuning ranges of three different working stages under different heatsink temperatures, and the lasing wavelength was not continuously tuned over the entire 95 nm coverage.

The above mentioned VECSELs with tuning range greater than 40 nm need either complex quantum design (which also means sophisticated epitaxial growth) of the active region or removing the DBR on the bottom of the gain chip (which is at the expense of the simplicity, compactness, stability, and reliability of a VECSEL). Similarly, it needs a specially designed wideband gain chip along with significantly changed operating temperature of the laser to change the lasing wavelength substantially and obviously expand the tuning range.

We report a widely tunable VECSEL based on a usually designed gain chip and a simple straight-line cavity. Different tuning elements are used to obtain continuous tuning of the laser wavelength, and the maximum tuning range of 45 nm is performed. For the first time, we propose an easily available blade as the tuning element in the cavity, and a wavelength tuning range more than 10 nm is demonstrated. These tunable VECSELs can meet the demands of most practical applications, while the simplicity, compactness, stability, and reliability of the laser are still maintained.

2. GAIN CHIP AND ITS PHOTOLUMINESCENCE CHARACTERISTICS

The gain chip used in the experiment is epitaxially grown in reverse sequences. First, an etch stop layer of AlGaAs with high Al composition is deposited on the GaAs substrate, then a protect layer of GaAs is grown. An AlGaAs layer with high barrier to prevent the carriers from surface recombination comes next, and following is the active region consisting of multiple quantum wells. There are 12 InGaAs/GaAsP quantum wells in the active region, and the content of In in InGaAs is designed to meet the target laser wavelength of 976 nm. Since the GaAsP layer would play three roles (i.e., the strain compensation layer, the barrier layer, and the pump absorption layer) in the active region, the content of P in GaAsP must be adequate to compensate the strain and cannot be too much to absorb the pumping energy.

Above the active region is the DBR, which is composed of 30 pairs alternate of AlGaAs layers with high Al (lower refractive index) and low Al (higher refractive index) composition. The designed center wavelength and high-reflectivity bandwidth of the DBR are 976 and 100 nm, respectively. The entire epitaxial wafer is ended by an antioxidant GaAs layer. In a VECSEL, the DBR at the bottom and the semiconductor–air interface at the front of the chip form a microcavity, and this will result in a laser standing wave in the active region. To get a higher gain coefficient, the thickness of every single layer in the wafer, especially layers of multiple quantum wells, should be designed and grown accurately to ensure that all quantum wells are located at the peaks of the standing wave to form a resonant periodic gain structure [26].

The grown wafer is split into small chips with 4 mm × 4 mm dimensions. The epitaxial end face of the chip is metalized with titanium-platinum-aurum sequentially, then the chip is bonded to a copper heatsink, and the substrate is removed using chemical etch.

Photoluminescence (PL) spectra carry much direct or indirect information of the epitaxial quality of the gain chip, e.g., whether the composition and thickness of quantum wells in the active region meet the design targets, if the thicknesses of other epitaxial layers are accurate, and whether or not the overall structure of the active region matches the requirements of resonant periodic gain structure. In addition, because the emission wavelength of semiconductor materials is very sensitive to temperature, PL spectra are often used to characterize the thermal dissipation of the entire gain chip.

It should be mentioned that there are two kinds of PL spectrum, the edge-emitting and the surface-emitting PL spectrum. The former reflects the PL characteristics of quantum wells in the active region directly and can be collected at any side of the four sides of the gain chip, while the latter can be regarded as an edge-emitting PL spectrum that has been modulated by the multilayer structure of the chip [27]. Different from the edge-emitting PL spectrum, a surface-emitting PL spectrum directly reflects the cavity mode of the semiconductor microcavity instead of the luminescence characteristics of the quantum wells, and it can be easily measured on the front side perpendicular to the surface of the gain chip. The PL spectrum below refers to the surface-emitting PL spectrum.

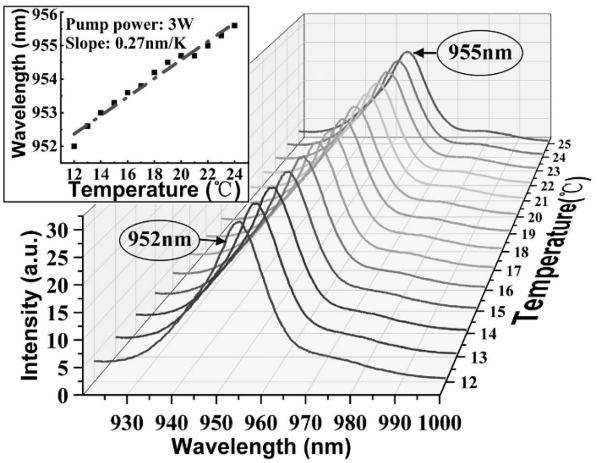

Fig. 1. PL spectra of the gain chip with different heatsink temperatures. The inset shows the slope of peak wavelengths of PL spectra versus temperatures.

For a gain chip based on GaAs material system, the microcavity mode will redshift at a rate of about 0.1 nm/K with increasing temperature because of the temperature-caused change of the material refractive index. Figure 1 shows the PL spectra of the gain chip with different heatsink temperatures when the pump power is 3 W. The slope of peak wavelengths of the PL spectra (can also be understood as the cavity modes of the semiconductor microcavity) versus heatsink temperatures, as can be seen from the inset on the left of Fig. 1, is about three times bigger than the typical value of 0.1 nm/K for a GaAs-based material system. This value means that the actual temperature in the active region is approximately three times higher than the temperature of the heatsink, i.e., for the gain chip, the heat dissipation is less efficient and the thermal effect is rather serious, which would limit the output power of the laser significantly. The marked peak emission wavelength is centered at 955 nm under a condition of 25 °C heatsink temperature and 3 W pump power. Obviously, it is 21 nm shorter than the target wavelength of 976 nm, and this is another factor limiting the output power of our VECSEL.

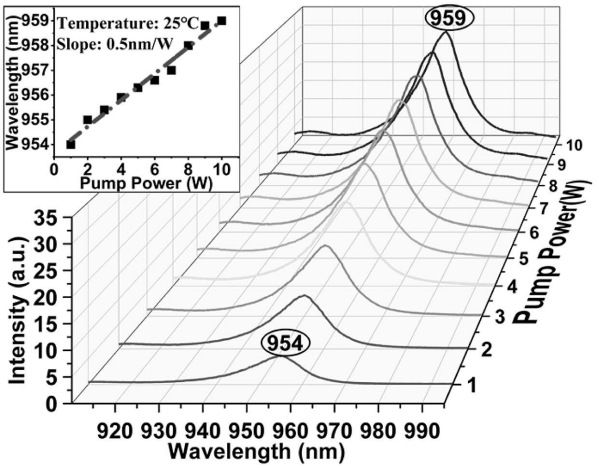

Fig. 2. PL spectra of the gain chip under various pump powers. The inset shows the slope of peak wavelengths of PL spectra versus pump powers.

Similarly, we plot the PL spectra of the gain chip under various pump powers with 25°C temperature in Fig. 2, and the inset shows the slope of peak wavelengths of the PL spectra versus pump powers. The value of 0.5 nm/W suggests that the temperature in the active region will rise by 5°C with the increase of 1 W pump power. When the pump power reaches 10 W, the peak wavelength redshifts 5 nm, and the estimated temperature rise in the active region arrives at 50°C.

3. TUNABLE OUTPUT

We test the output performances of the free-running VECSEL before its tunable operation is implemented. As shown in Fig. 3, a simple straight-line cavity is built, and a high-reflectivity (99.9% reflectivity at 980 nm) coated plane-concave mirror with 100 mm radius of curvature is chosen as the output coupler (OC). The pumping source, an 808 nm fiber coupled output semiconductor laser, is collimated by a 1:1 imaging lens pair and then focused on the gain chip at an incident angle of about 30°. Since the core diameter of the fiber is 200 μm, the cavity length is chosen to be about 95 mm to make the laser spot on the gain chip match the pump spot.

Figure 4 shows the output powers as a function of pump powers for the free-running VECSEL with fundamental transverse mode under room temperature. The lasing threshold is approximately 2.5 W, the maximum output power is 0.58 W, and the slope efficiency (SE) is 7%. We believe that the rather serious thermal effect mentioned before, the epitaxial deviation from the design target wavelength, as well as the relatively small transmittance of OC are the three main factors limiting the output power and lowering the SE of the laser. We have found out from Fig. 2 that the estimated temperature rise in the active region will arrive at 50 °C when the pump power is close to 10 W, and this is consistent with the case in Fig. 4. It is clear that the 50 °C temperature will decrease the material gain of quantum wells greatly and drop the output power of the laser significantly when the pump power approaches to 10 W.

Because of the good mode discrimination, the continuous tuning, the small insert loss, and the wide tuning range, BRFs are frequently used in a laser as the tuning element. In our experiment, three different BRFs with thicknesses of 2, 4, and 6 mm are employed, and the corresponding tuning characteristics are depicted in Figs. 5, 6 and 7, respectively.

After the test of the free-running VECSEL has been done, an uncoated 2 mm thickness fused quartz BRF is placed into the straight-line cavity at Brewster's angle, and the tuning curve under room temperature is shown in Fig. 5. When the BRF is rotated around the central axis perpendicular to its surface, the wavelength can be continuously tuned from 943 to 988 nm, indicating a wavelength coverage of 45 nm. As shown in Fig. 5,

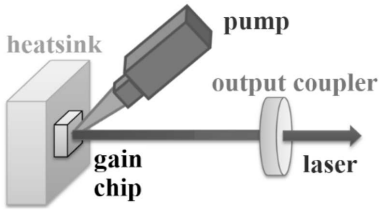

Fig. 3. Schematics of the experiment.

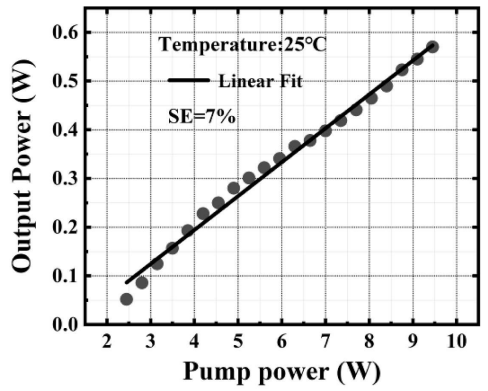

Fig. 4. Output powers as a function of pump powers for the free-running VECSEL.

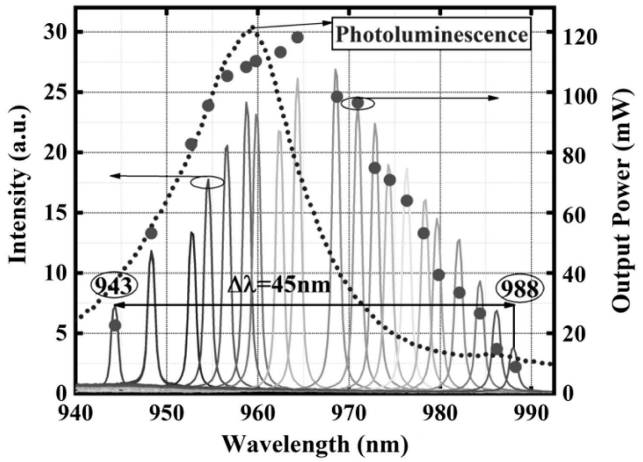

Fig. 5. Tuning characteristics including output powers and wavelengths of the VECSEL with a 2 mm thickness BRF. The dotted line is the PL spectrum of the gain chip under the same heatsink temperature and pump power.

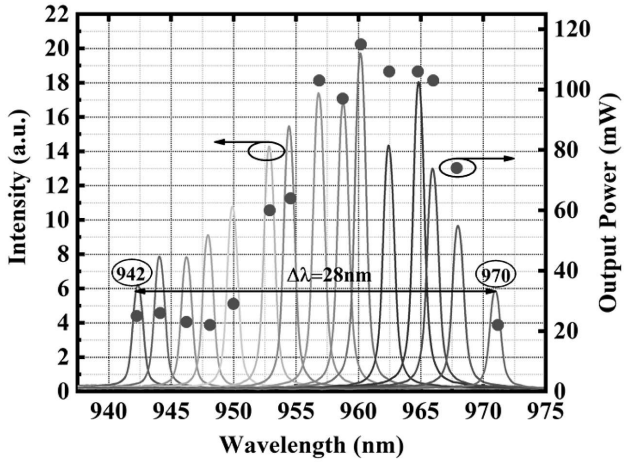

Fig. 6. Tuning characteristics of the VECSEL with a 4 mm thickness BRF.

the maximum output power is 120 mW at the center wavelength of 964 nm, and the minimum power is about 10 mW at the longest wavelength of 988 nm when the pump power is set to

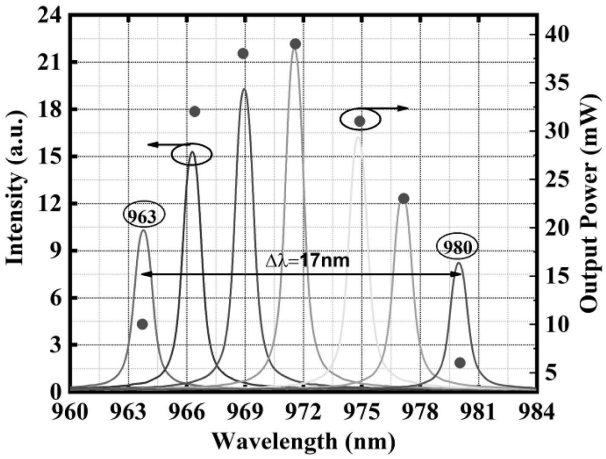

Fig. 7. Tuning characteristics of the VECSEL with a 6 mm thickness BRF.

8.4 W. Compared with the case of free running (about 480 mW output power versus 8.4 W input power), the maximum output power of the tunable laser is reduced by a factor of 3/4, which is mainly resulted from the insert loss of the BRF. A dotted line representing the PL spectrum of the gain chip under the same pump power and room temperature is also plotted in Fig. 5. It is shown that the output power of the tunable laser has a similar outline of the PL spectrum in roughly the same wavelength range, and this make sense if we consider that the mode gain of a laser has a comparable outline to its PL spectrum.

The tuning equation of a BRF is

$$\lambda = \frac{(n_o - n_e)d\ \sin^2\gamma}{m\sin\theta_b} = C_0(1 - \cos^2\phi\cos^2\theta_b), \quad (1)$$

where $n_o - n_e$ is the refractive index difference, d is the thickness of filter, γ is the angle between the refractive ray and the crystal's optical axis, m is the interference level, θ_b is the Brewster's angle. For $C_0 = (n_o - n_e)d\,/m\sin\theta_b$, ϕ is the angle between the crystal's optical axis and the incident surface, i.e., the tuning angle. According to the above equation, when the wavelengths are tuned from 943 to 988 nm in Fig. 5, the tuning angle can be varied between 6° and 70° under different interference-level values of m.

The tuning characteristics including the changed wavelengths and the corresponding output powers of the VECSEL with 4 and 6 mm thickness BRF are shown in Figs. 6 and 7, respectively. It can be concluded from the figures that the tuning range and the maximum output power of the tunable laser all decrease with increasing thickness of the BRF. The tuning ranges of the VECSEL with 2, 4, and 6 mm thickness BRF are 45, 28, and 17 nm, respectively, while their maximum output powers are 120, 113, and 38 mW.

For a BRF, the wavelength tuning range, i.e., the free spectral range (FSR) can be expressed as

$$\Delta\lambda_F = \frac{\lambda^2}{\Delta n d}, \quad (2)$$

where λ is the laser wavelength, $\Delta n = n_o - n_e$ is the birefringence index difference of quartz material, which has a typical value of 9×10^{-3}, and d is the thickness of BRF. The above

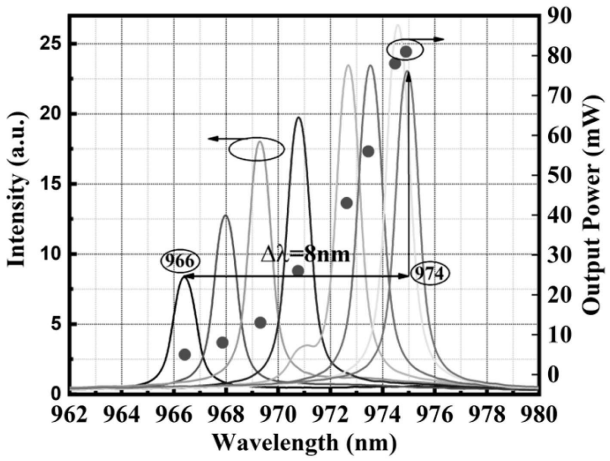

Fig. 8. Tuning characteristics of the VECSEL by the use of a 0.15 mm thickness uncoated FP etalon.

formula predicts a decreasing tuning range of BRF with increasing thickness, which is identical with Figs. 5–7. Theoretically, thinner BRF can produce a larger tuning range. However, in an actual tunable laser, the wavelength tuning range not only depends on the thickness of the BRF but also relates to the bandwidth of the gain medium. In fact, most of the tuning range provided by BRF is beyond the need of the experiment itself. For example, the free spectrum range of the 2 mm thick quartz BRF used in our experiment is 102.4 nm, which has exceeded the gain bandwidth and even the fluorescence spectrum width of the chip. It also should be noted that the output laser is a polarized beam because the BRF is placed into the cavity at Brewster's angle.

Besides BRFs, Fabry–Perot (FP) etalons are also widely used as intracavity tuning elements to adjust the output wavelength of a laser. However, the insert loss of an etalon is relatively higher, and its FSR is much smaller than that of a BRF. In addition, its mode discrimination ability is not as good as a BRF, so the tuning of the laser wavelength is often not continuous, and mode hopping may happen during the tuning process. Figure 8 shows the tuning characteristics of the VECSEL using a 0.15 mm thickness uncoated FP etalon and that the laser wavelength can be tuned monotonically to the short wavelength direction. The maximum output power of the tunable laser is about 80 mW, and the wavelength tuning range is 8 nm.

Although their work mechanism is completely different (BRFs use the interference of polarized light, FP etalons use the interference of multibeam), in terms of the final effect, we can always think that the reason why BRF and FP etalon can tune the wavelength is that when their position or attitude in the cavity is changed, they have different transmittance for different wavelengths. In other words, they have different losses for various wavelengths. According to the same principle, we propose the following method to tune the laser wavelength by using a blade as the loss-adjustable element.

In a VECSEL with a straight-line cavity, the size of the laser spot at any position in the cavity satisfies the formula

$$\omega^2 = \frac{4\lambda L}{\pi}\sqrt{L/(R-L)}, \tag{3}$$

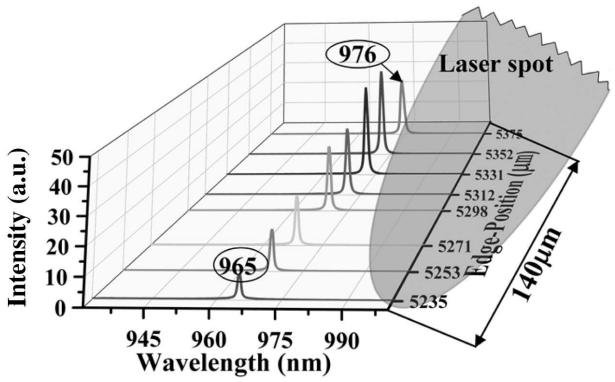

Fig. 9. Tuning performances of the VECSEL using a blade as the tuning element.

where λ is the laser wavelength, L is the length of the observation point from the gain chip, and R is the curvature radius of the output coupler. Obviously, the laser mode with longer wavelength will have larger spot size. Therefore, if an aperture (can be in any form) is placed into the resonator, the insert loss for a laser mode with longer wavelength is bigger than that for a laser mode with shorter wavelength when the diameter of the aperture is decreased gradually. Then, the mode competition will force the laser wavelength to change to a shorter value to meet the requirement of oscillation, and the output wavelength thus can be tuned along the short wavelength direction in a certain range. It should be noticed that for better mode discrimination, the laser spot should be as big as possible, i.e., the inserted aperture should be as near to the OC as can as possible.

Here we use a blade as a half-slit aperture. When the blade is inserted perpendicularly into the cavity and moved gradually to the optical axis, the laser wavelength can be tuned continuously from the initial longer wavelength to the eventual shorter wavelength. Figure 9 shows the performance of the tunable VECSEL using the above method. The x axis represents the laser wavelength, the y axis represents the spectral intensity, and the z axis indicates the relative position (which is directly read from a one-dimensional translation stage used to fix the blade) of the blade. As shown in Fig. 9, the laser wavelength is changed from the first longer 976 nm to the last shorter 965 nm when the blade is moved to the optical axis (i.e., the center of a laser spot) over a distance of 140 μm. After that, too deep of an insert of the blade, which means too much intracavity loss of the laser, means the laser cannot maintain the oscillation any more. The obtained wavelength coverage is 11 nm, wider than that of the laser with 0.15 mm thickness FP etalon but narrower than that of the laser with 2 mm thickness BRF.

For a Gaussian beam whose intensity satisfies the following equation:

$$I(\mathrm{r}) = I_0 \exp\left(-\frac{2r^2}{\omega^2}\right), \tag{4}$$

where I_0 is a constant, r is the radial coordinate, and ω is the radius of the beam waist, the transmittance of a Gaussian beam through an aperture with radius of C can be expressed as

$$T = \frac{\int_0^C \int_0^{2\pi} I(r) 2\pi r \mathrm{d}r \mathrm{d}\theta}{\int_0^\infty \int_0^{2\pi} I(r) 2\pi r \mathrm{d}r \mathrm{d}\theta}. \tag{5}$$

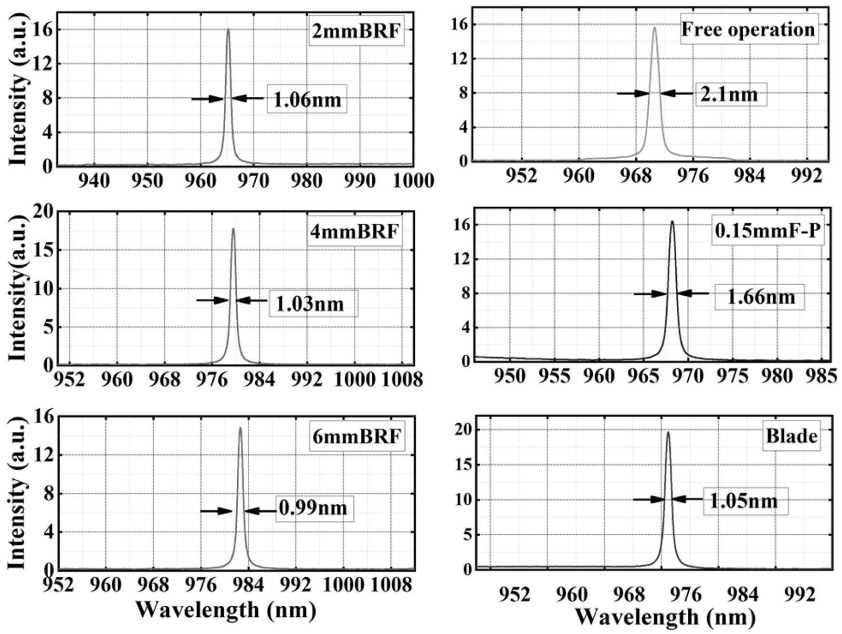

Fig. 10. Laser spectra of the free-running VECSEL and the tunable VECSELs with different tuning elements.

It can be estimated that when the blade is inserted to 140 μm, the transmission rate is reduced by 36% compared to the initial uninserted blade.

Finally, we pay attention to the laser linewidth of the free-running VECSEL and tunable VECSELs with different tuning elements, and the results are shown in Fig. 10. It can be concluded from Fig. 10 that when a BRF or a blade is used, the laser linewidth obviously decreases to about half of that of a free-running VECSEL. However, when a 0.15 mm FP etalon is employed as the tuning element, the reduction of laser linewidth is not very clear. The three parts on the left side of Fig. 10 indicate that in the VECSELs with a BRF, the linewidth of the output laser decreases with the increasing BRF thickness, but the change is not significant. The smaller laser linewidth of a BRF or FP etalon tuning VECSEL can be easily understood because the BRF or FP etalon itself has the effect of narrowing the laser linewidth. As for a blade-tuning VECSEL, when a blade is inserted into the resonant cavity, it works as a half-slit aperture, so to limit the size of the laser transverse mode further partly improves the longitudinal mode of the laser, because the inserted blade reduces the transverse mode of the laser in the cavity as well as the laser spot on the gain chip. This will improve the uniformity of the lasing region in the gain chip, reduce the line broadening of the laser, and produce a narrower output laser spectrum.

4. CONCLUSIONS

In summary, we have demonstrated tunable VECSELs with various methods. When a BRF is used as the tuning element, the range of changeable laser wavelength decreases with the increasing BRF thickness. The maximum tuning range of 45 nm and the maximum output power of 120 mW are obtained from a VECSEL with 2 mm thickness uncoated fused silica BRF. The oscillating wavelength can be tuned over an 8 nm range by using a 0.15 mm thickness FP etalon. Particularly, we propose a method employing an easily available blade as the tuning element to adjust the lasing wavelength. The output wavelength of the laser can be tuned from the initial longer wavelength to the final shorter wavelength continuously, and the wavelength coverage is more than 10 nm. The BRF method can produce the widest tuning range of 45 nm, and further extension of the wavelength coverage needs a gain chip with wider gain spectrum, such as a gain chip that consists of QD material or quantum wells with different composition or different well width. The presented tunable VECSEL only needs a generally designed gain chip and uses the simplest, most compact, and most stable straight-line cavity. It has great application value in cases where miniaturization, stability, reliability, hundreds of milliwatts of output power, and tens of nanometers of tuning range of the laser are highly demanded.

Funding. Scientific and Technological Research Program of Chongqing Municipal Education Commission (KJQN201800528); State Key Laboratory of Luminescence and Applications (SKLA-2019-04); "Blue Fire Plan" (Huizhou) Foundation of Industry University Research Joint Innovation of Ministry of Education (CXZJHZ201728); Chongqing Research Program of Basic Research and Frontier Technology (cstc2018jcyjAX0319); National Natural Science Foundation of China (61904024); Fundamental Research Funds for the Key Research Program of Chongqing Science and Technology Commission (KJZD-M201900502).

Disclosures. The authors declare no conflicts of interest.

Data Availability. Data underlying the results presented in this paper are not publicly available at this time but may be obtained from the authors upon reasonable request.

REFERENCES

1. B. Lu, F. Wei, Z. Zhang, D. Xu, Z. Q. Pan, D. J. Pan, D. J. Chen, and H. W. Cai, "Research on tunable local laser used in ground-to-satellite coherent laser communication," Chin. Opt. Lett. **13**, 091402 (2015).

2. T. Farrell and D. McDonald, "Tunable laser technology for sensing applications," Proc. SPIE **5594**, 66–80 (2004).
3. A. N. Soldatov, I. V. Reimer, V. A. Evtushenko, K. Y. Melnikov, and A. V. Malikov, "Tunable wavelength laser medical system for treating oncological diseases," Bull. Lebedev Phys. Inst. **37**, 4–5 (2010).
4. K. W. Rothe, U. Brinkmann, and H. Walther, "Applications of tunable dye lasers to air pollution detection: measurements of atmospheric NO_2 concentrations by differential absorption," Appl. Phys. **3**, 115–119 (1974).
5. K. N. Wang, T. Cui, L. V. Qian, and K. G. Gao, "Enhanced lasing behavior enabled by guided-mode resonance structure embedded with double waveguide layers," Appl. Opt. **59**, 6113–6118 (2020).
6. P. S. Bhatia and J. W. Keto, "Precisely tunable, narrow-band pulsed dye laser," Appl. Opt. **35**, 4152–4158 (1996).
7. Y. R. Guo, M. Z. Xu, W. N. Peng, J. Su, H. D. Lu, and K. C. Peng, "Realization of a 101 W single-frequency continuous wave all-solid-state 1064 nm laser by means of mode self-reproduction," Opt. Lett. **43**, 6017–6020 (2018).
8. P. X. Jin, H. D. Lu, Q. W. Yin, J. Su, and K. C. Peng, "Expanding continuous tuning range of a CW single-frequency laser by combining an intracavity etalon with a nonlinear loss," IEEE J. Sel. Top. Quantum Electron. **24**, 1–5 (2017).
9. J. Wei, X. C. Cao, P. X. Jin, J. Su, H. D. Lu, and K. C. Peng, "Diving angle optimization of BRF in a single-frequency continuous-wave wideband tunable titanium:sapphire laser," Opt. Express **29**, 6714–6725 (2021).
10. Q. W. Yin, H. D. Lu, J. Su, and K. C. Peng, "High power single-frequency and frequency-doubled laser with active compensation for the thermal lens effect of terbium gallium garnet crystal," Opt. Lett. **41**, 2033–2036 (2016).
11. R. L. Byer, "Diode laser-pumped solid-state lasers," Science **239**, 742–747 (1988).
12. G. Huber, C. Krnkel, and K. Petermann, "Solid-state lasers: status and future [Invited]," J. Opt. Soc. Am. B **27**, B93–B105 (2010).
13. M. Kuznetsov, F. Hakimi, R. Sprague, and A. Mooradian, "High-power (0.5-W CW) diode-pumped vertical-external-cavity surface-emitting semiconductor lasers with circular TEM00 beams," IEEE Photon. Technol. Lett. **9**, 1063–1065 (1997).
14. A. C. Tropper and S. Hoogland, "Extended cavity surface-emitting semiconductor lasers," Prog. Quantum Electron. **30**, 1–43 (2006).
15. A. Rahimi-Iman, "Recent advances in VECSELs," J. Opt.-UK **18**, 093003 (2016).
16. M. Guina, A. Rantamäki, and A. Härkönen, "Optically pumped VECSELs: review of technology and progress," J. Phys. D **50**, 383001 (2017).
17. B. Rudin, A. Rutz, M. Hoffmann, D. J. H. C. Maas, A. R. Bellancourt, E. Gini, T. Südmeyer, and U. Keller, "Highly efficient optically pumped vertical-emitting semiconductor laser with more than 20 W average output power in a fundamental transverse mode," Opt. Lett. **33**, 2719–2721 (2008).
18. B. Heinen, T.-L. Wang, M. Sparenberg, A. Weber, B. Kunert, J. Hader, S. W. Koch, J. V. Moloney, M. Koch, and W. Stolz, "106 w continuous-wave output power from vertical-external-cavity surface-emitting laser," Electron. Lett. **48**, 516–517 (2012).
19. J. Y. Zhang, J. W. Zhang, Z. Zhang, Y. G. Zeng, X. Zhang, H. B. Zhu, Y. W. Huang, L. Qin, Y. Q. Ning, L. J. Wang, and J. J. Cui, "High-power vertical external-cavity surface-emitting laser emitting switchable wavelength," Opt. Express **28**, 32612–32619 (2020).
20. L. Fan, M. Fallahi, J. T. Murray, R. Bedford, Y. Kaneda, A. R. Zakharian, J. Hader, J. V. Moloney, W. Stolz, and S. W. Koch, "Tunable high-power high-brightness linearly polarized vertical-external-cavity surface-emitting lasers," Appl. Phys. Lett. **88**, 021105 (2006).
21. L. Fan, M. Fallahi, A. R. Zakharian, J. Hader, and S. W. Koch, "Extended tunability in a two-chip VECSEL," IEEE Photon. Technol. Lett. **19**, 544–546 (2007).
22. C. Borgentun, J. Bengtsson, A. Larsson, F. Demaria, A. Hein, and P. Unger, "Optimization of a broadband gain element for a widely tunable high-power semiconductor disk laser," IEEE Photon. Technol. Lett. **22**, 978–980 (2010).
23. M. Butkus, J. Rautiainen, O. G. Okhotnikov, C. J. Hamilton, G. P. Malcolm, S. S. Mikhrin, I. L. Krestnikov, D. A. Livshits, and E. U. Rafailov, "Quantum dot based semiconductor disk lasers for 1–1.3 μm," IEEE J. Sel. Top. Quantum **17**, 1763–1771 (2011).
24. Z. Yang, A. R. Albrecht, J. G. Cederberg, and M. Sheik-Bahae, "80 nm tunable DBR-free semiconductor disk laser," Appl. Phys. Lett. **109**, 1063 (2016).
25. B. Artur, W. J. Anna, S. Iwona, W. Michal, W. Marta, and M. Jan, "A 95-nm-wide tunable two-mode vertical external cavity surface-emitting laser," IEEE Photon. Technol. Lett. **29**, 2215–2218 (2017).
26. M. Y. A. Raja, S. R. Brueck, M. Osinski, C. F. Schaus, J. G. McInerney, T. M. Brennan, and B. E. Hammons, "Resonant periodic gain surface-emitting semiconductor lasers," IEEE J. Quantum Electron. **25**, 1500–1512 (1989).
27. P. Zhang, T. Dai, Y. Liang, S. Fan, Y. Song, and X. Zhang, "Spectral characteristics of amplified spontaneous emission in a semiconductor disc laser," J. Phys. D **45**, 235103 (2012).